Nucleation probability of methane + propane mixed-gas hydrate depending on gas composition

*Tsutomu Uchida**[1], *Masato Hayama*[2], *Motoi Oshima*[3], *Kenji Yamazaki*[1],

[1]Division of Applied Physics, Faculty of Engineering, Hokkaido University, Sapporo 060-8628, Japan

[2]Division of Applied Physics, Graduate School of Engineering, Hokkaido University, Sapporo 060-8628, Japan

[3]Methane Hydrate Production Technology Research Group, Energy Process Research Institute, Department of Energy and Environment, National Institute of Advanced Industrial Science and Technology (AIST), Sapporo 062-8517, Japan

* Corresponding Author

E-mail: t-uchida@eng.hokudai.ac.jp (T. U.), orcid.org/0000-0003-2304-376X

KEYWORDS: induction time, nucleation probability, methane-propane mixed gas hydrate, composition dependence, blob model

ABSTRACT

Gas hydrates show promise as gas storage and transportation media. But before using them in such industries, we should learn how to better control their formation. In particular, their nucleation is stochastic and requires either high supersaturations or long induction times. Here we study experimentally how the induction time varies with the gas composition using methane (CH_4) + propane (C_3H_8) mixed-gas hydrate as a mimic of natural gas. We form CH_4 + C_3H_8 mixed-gas hydrates with a composition ratio CH_4:C_3H_8 ranging from 100:0 to 0:100 in a high-pressure vessel with a stirring system at a constant temperature of about 274.7 K. The induction time is determined as the time period from the start of stirring to the hydrate formation defined by either a sudden temperature rise or a pressure drop in the vessel. To obtain quantitative nucleation data, we repeat at least 10 experiments for each condition. Compared to that of pure CH_4 hydrate, the induction time of CH_4 + C_3H_8 mixed-gas hydrate is found to be significantly shorter when C_3H_8 is present at even 1% in the vapor. Then, we quantify the stochastic nucleation process as the composition-dependent nucleation frequency. As a result, we show that the nucleation frequency of CH_4 + C_3H_8 mixed-gas hydrate exponentially decreases with increasing C_3H_8 in vapor. This behavior correlates well with the composition dependence of the empty-cage ratio in the gas hydrate. Based on these results, we propose a model for the nucleation of mixed-gas hydrates.

(243/300 words)

I. Introduction

Gas-hydrate crystallization is a possible way to store and transport natural gases. For industrial use, we need better technology for promoting gas-hydrate crystallization. Most gas-hydrate research has historically targeted the prevention of hydrate formation because hydrates that form in gas pipelines cause blockage,[1,2] with relatively little research targeting the promotion of hydrate crystallization.[3-16] For crystallization, one problem is the random nature of the nucleation process. As is the case with ice, nucleation of gas hydrate requires either a high supercooling or a long induction time, increasing the difficulty of experimental studies. Thus, there are relatively few experimental studies of hydrate nucleation.[1,2,12,17-21]

Through experimental and simulation approaches, several nucleation mechanisms have been proposed.[2,18,22] For example, Sloan et al.[23,24] proposed the labile-cluster hypothesis, which proposes that nucleation begins when water molecules form a cage-like structure around the guest molecules. Presumably, during this initial stage the cage structure that develops must be large enough to encompass the guest molecular. For example, the smaller 5^{12}-cage-like cluster will form around the smaller CH_4 molecule, whereas the larger $5^{12}6^4$-cage-like cluster will form around the larger C_3H_8 molecule. Such size selection will apply to all mechanisms. A later mechanism to be proposed argues that nucleation occurs at an interface, for example, at the gas-liquid interface.[25,26] Another mechanism is based on local structure, assuming that the structuring of guest molecules induces nucleation.[27] The above models all presume single-guest hydrate nucleation and focus on the initial stage in which isolated cages form. As such, the assembly of the cages into the final lattice must be considered separately.

A recent model that also applies to mixed gas hydrates is the blob model, a model that assumes nucleation begins from an amorphous precursor.[28,29] This concept has been developed as a two-step formation model in which an amorphous precursor changes to a crystalline structure.[30-32] Even more recent is the multi-pathway nucleation model.[33] This model assumes

that several processes occur in combination. However, there is still a knowledge gap in comparing these models with macroscopic phenomena observed in the laboratory.

Several methods have been proposed to promote gas-hydrate nucleation, such as adding surfactants[34-39] and solid particles,[37,40-49] but these methods have economic and environmental drawbacks. Instead, a technique that uses the memory effect, a property unique to gas hydrates, has attracted attention as a sustainable method.[50-56] The memory effect is a phenomenon in which the time required for nucleation is shorter when gas hydrates are formed using water in which they have been decomposed than using pure water.[1,2] As for the mechanism of the memory effect, several hypothesis have been proposed, such as the water-structuring hypothesis,[57,58] which states that a hydrate-like water-network structure remains in the water, and the gas-dissolved hypothesis,[59] which states that guest molecules remain in the water in a supersaturated state. Uchida et al.[54,60-63] found that the presence of ultra-fine bubbles formed when gas hydrates dissociate induces the memory effect for single-gas hydrates.[54] They then extended their research to the nucleation of mixed-gas hydrates using a methane (CH_4) + propane (C_3H_8) mixed gas, and found that nucleation occurred more quickly with mixed gases than with single gases despite the memory effect.[64] This means that it is difficult to predict the nucleation of mixed gases based on models for single-gas hydrates. They also found that the nucleation occurred more quickly at a higher supersaturation, which is consistent with supersaturation being the driving force of crystal growth.[64]

Although bulk CH_4 + C_3H_8 mixed gas hydrate with any amount of C_3H_8 should have structure type II (sII) in equilibrium,[65] the nucleus may initially have a less stable structure according to the Ostwald step rule. For example, several experimental and simulation studies on the nucleation of mixed-gas hydrate have reported a coexistence of both sI and sII structures in the early stages of formation.[13-16,66-71] Simulation studies have predicted several features of the nucleation processes of sII gas hydrate, such as nucleation being more rapid at higher C_3H_8

concentrations,[68] that the formation of empty cages as well as guest-occupied cages is important,[69] and that the occupancy of 5^{12} cages by CH_4 is observed before the formation of the sII structure.[70] In this study, we investigate the nucleation mechanism of mixed-gas hydrates by systematically examining the gas-composition influence on the nucleation of CH_4 + C_3H_8 mixed-gas hydrate.

II. Experimental Procedures

To ensure data consistency and allow a firmer comparison to previous studies, we use the same experimental method and apparatus as that in our previous study.[64] We now briefly describe this method.

We used ion-exchanged pure water of resistivity about 15 MΩ cm. The sample gas was a mixture of high-purity CH_4 (99.99%) and C_3H_8 (99%) gas (Hokkaido Air Water, Hokkaido, Japan). The composition was CH_4:C_3H_8 = 100:0 to 0:100. Data for pure C_3H_8-hydrate were taken from a previous study.[62] A high-pressure vessel (232.2 cm^3 in volume) equipped with a stirrer was submerged in a constant-temperature bath to maintain an experimental temperature of 274.2 ± 1.0 K. After introducing about 50 cm^3 of pure water, pure CH_4 and C_3H_8 gases were introduced to the target partial pressure by considering a set composition. The initial total pressure P_0 was selected at twice the equilibrium pressure P_d for the composition as calculated with the CSMHYD program[72] (i.e., supersaturation $\sigma = P_0/P_d - 1 = 1$). To test the composition of the source mixed-gas, we sampled a small amount of gas from the high-pressure vessel before the experiment and measured the composition using gas chromatography (GC-2014, Shimadzu, Kyoto, Japan) with a column of Sunpak-A 50/80 mesh (Shinwa Chemical Ind., Kyoto, Japan). The values measured by gas chromatography were used to analyze the results. For one case (CH_4:C_3H_8 = 99:1 mixed gas), accurate adjustment by partial pressure was difficult, so a standard gas (Hokkaido Air Water) was used instead.

The gas-hydrate formation tests began with an agitation of about 300 rpm. Temperature and pressure were measured by a data logger (GL-240, Graphtech, Kanagawa, Japan) every 5 s. The induction time (t_{ind}) is defined as the time interval from the start of agitation to the time of nucleation $t = t_f$ when we detected either a temperature rise or a pressure drop due to the subsequent growth of bulky gas-hydrate crystal. This series of experiments was repeated more than 10 times under the same conditions, exchanging the fresh water every time to eliminate any memory effect coming from the sample. To effectively eliminate any memory effect from the equipment, we also took the following steps. The reaction vessel was retrieved from the temperature bath at each experimental interval, and then the inside of the vessel was thoroughly dried and brought to room temperature by airing out with forced ventilation for several hours. When no such nucleation occurred within 50 h (3000 min), we classified the case as "no nucleation".

As to the location of nucleation, we could not observe the hydrate directly and thus could not determine whether or not the nucleation occurred at an interface.

As t_f differs for each experiment, the temperature and pressure at nucleation are not the same as the initially set conditions. We then use the temperature T_f and pressure P_f immediately before nucleation to represent the nucleation conditions for each sample, and assume that the variations in T_f and σ between the repeated experiments provide a measure of the uncertainty because they are larger than those of measurement accuracies. To evaluate the nucleation phenomenon quantitatively, the fraction of trials that nucleate within a given t_{ind} is considered to be the nucleation probability. The cumulative t_{ind} curve is the nucleation probability distribution $\Pi(t)$, which is fitted to equation (1) below[73,74] using commercially supplied software (Origin Pro 9.0, Light Stone):

$$\Pi(t) = 1 - \exp[-J(t - \tau_0)], \quad (1)$$

where J is the nucleation frequency and τ_0 the offset time. Generally, J is closely related to the nucleation rate and τ_0 generally scales with the minimum induction time.

III. Results

Figure 1 (a) shows the resulting nucleation probability distribution for the full range of compositions at temperature $T_f = 274.7$ K and supersaturation $\sigma = 0.99$. To aid comparison, the data for pure CH_4 hydrate (this study) are connected with a dark solid line, whereas that for pure C_3H_8 hydrate[64] are connected with a light hollow line. Several CH_4-rich cases are also connected. Figure 1 (b) shows the composition dependence (shown as the C_3H_8 concentration, x) of the induction time at 50% nucleation probability, which is shown as the cross point of each nucleation probability distribution curve and the horizontal line at the nucleation probability of 0.5 (light dotted line in Fig. 1(a)).

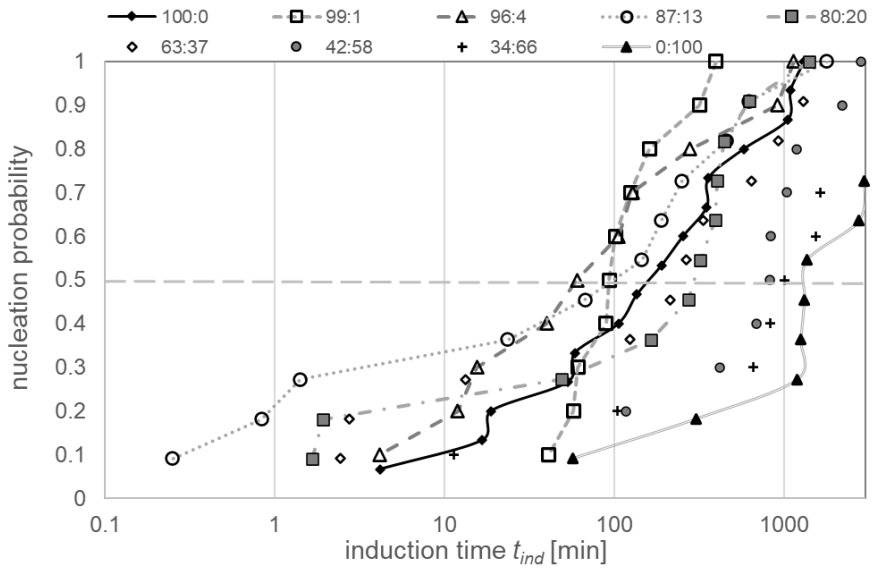

(a)

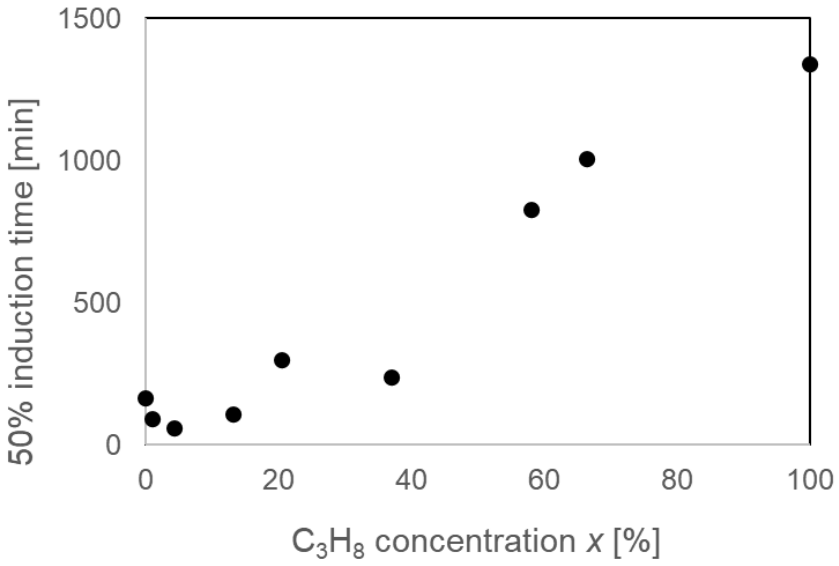

(b)

Fig. 1: (a) Nucleation probability distributions of CH_4 + C_3H_8 mixed gas hydrates of nine composition conditions (legend at top) at T_f = 274.7 ± 0.4 K and supersaturation σ = 0.99 ± 0.18. Dark solid line is pure CH_4 hydrate, light hollow line is pure C_3H_8 hydrate (from ref. 64), and dashed or dotted lines are mixed-gas cases with C_3H_8 below 20%. (b) The induction time at 50% nucleation probability for the full range of compositions.

Considering the trend with composition, Figs. 1(a) and (b) shows the nucleation probability distribution shifting to smaller t_{ind} with increasing CH_4 concentration (or decreasing C_3H_8 concentration), indicating that CH_4 promotes nucleation of the mixed-gas hydrate. Consistent with this trend, the nucleation probability distribution of pure C_3H_8 hydrate is smaller (longer t_{ind}) than those of any of the mixed-gas hydrates. However, in the other direction, when the concentration of C_3H_8 goes to zero, the nucleation probability distribution of pure CH_4 hydrate shifts to longer times than that of the mixed-gas hydrates containing less than 10% of C_3H_8. This trend is clearer in Fig. 1(b), where we plot the 50% induction time. In other words, the nucleation of CH_4 hydrate appears to be promoted by the presence of a small amount of C_3H_8.

Moreover, with the addition of small amounts of C_3H_8, the induction time t_{ind} spreads out. Times less than several minutes were even observed for the cases of CH_4:C_3H_8 = 87:13 and 96:4. However, in the case of CH_4:C_3H_8 = 99:1, the values of t_{ind} concentrate in the range of 40 to 400 min. Overall, it is clear that different compositions result in different patterns of nucleation probability distribution.

Using the fitting equation (1), we compiled the values of J for the full range of compositions, listing them in Table 1 and plotting the values in Fig. 2. For a useful comparison of the composition dependence, the supersaturations should all be the same. However, as the supersaturation changed during a given experiment (due to dissolution of gas in the water or the fluctuation of the temperature control system), the average supersaturation deviated from the initial value of $\sigma = 1$ (Table 1). Thus, to aid the comparison of the composition dependence, we also calculated a σ-corrected nucleation frequency $\langle J \rangle$ for the condition of $\sigma = 1$. For the calculation, we use the following relationship obtained in a previous study:[64]

$$J = \mathrm{K}\ \sigma^{\mathrm{n}} \quad , \qquad (2)$$

with K and n being obtained at the composition of CH_4:C_3H_8 = 90:10 and having the values[64] $\mathrm{K} = 5.5\times10^{-2}$ and n = 2.6. Although these values may vary with composition, here we assume they hold for all CH_4 + C_3H_8 mixed-gas hydrates (applied only for sII structures).

Table 1: Average formation conditions and fitting parameters.

CH_4	C_3H_8	P_f	T_f	σ	J	$\langle J \rangle$	τ_0	R^2
%	%	MPa	K		$\times 10^{-3}$ min^{-1}	$\times 10^{-3}$ min^{-1}	min	
100	0	5.77	274.7	0.902	2.33		–132	0.970
99	1	3.13	275.2	0.956	12.0	13.5	34	0.975
96	4	1.50	274.3	0.980	7.50	7.91	–21	0.956
87	13	1.07	274.4	0.906	5.24	6.77	–49	0.955
80	20	0.779	274.8	0.798	2.54	4.57	–51	0.940
63	37	0.637	274.6	0.815	1.95	3.32	–104	0.962
42	58	0.499	274.7	0.758	0.953	1.96	–67	0.941
34	66	0.432	274.7	0.812	0.550	0.945	–196	0.940
0	100	0.42	273.7	1.21	0.331	0.0201	–204	0.714

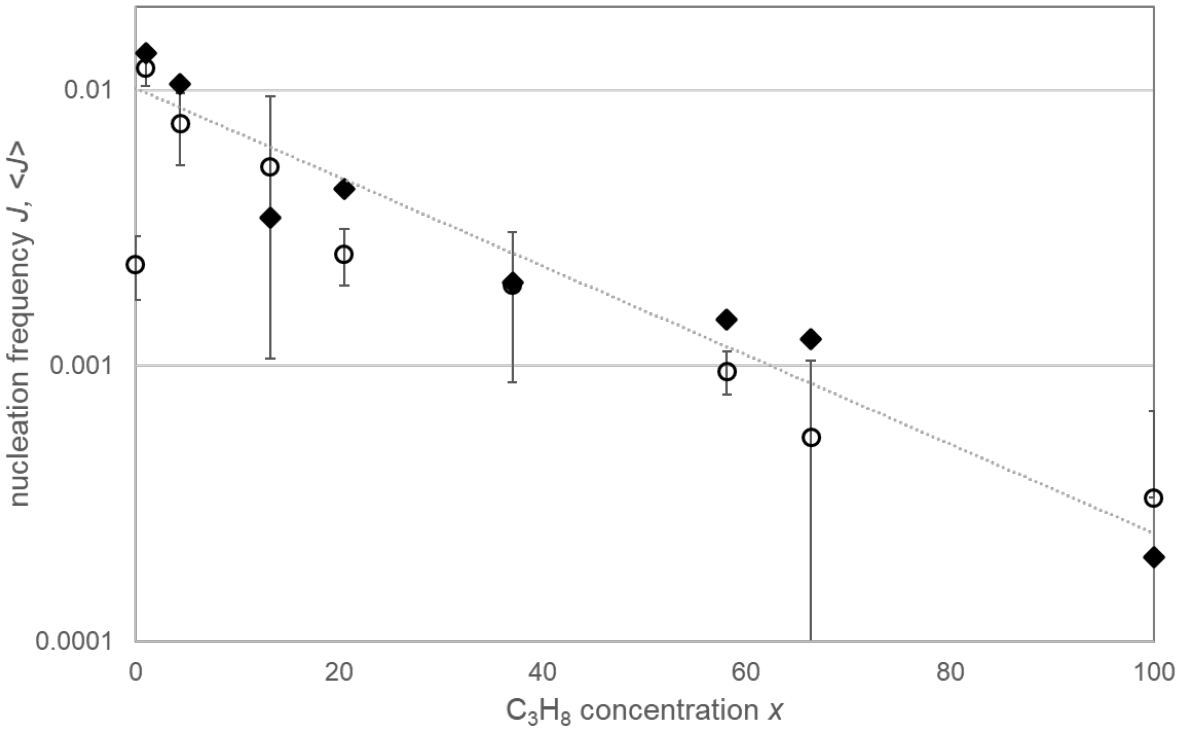

Fig. 2: Nucleation frequency J (open circles) and σ-corrected nucleation frequency $\langle J \rangle$ (solid diamonds) for a range of C_3H_8 concentrations in $CH_4 + C_3H_8$ mixed gas hydrates. No diamond is shown for $x = 0$ because that hydrate has the sI structure and thus is not used to estimate $\langle J \rangle$. The dotted line shows the regression line of equation (3).

As shown in Fig. 2, the value of $\langle J \rangle$ decreases with an increasing concentration of C_3H_8. For pure CH_4 hydrate, the value of J is nearly one order of magnitude smaller than that of the condition of 1% C_3H_8 containing mixed-gas hydrate. Except for pure CH_4 hydrate, therefore, the value of $\langle J \rangle$ decays exponentially with x, the concentration of C_3H_8 in $CH_4 + C_3H_8$ mixed-gas hydrates. This relationship is fit by the equation (3) ($R^2 = 0.88$):

$$\langle J \rangle = 1.0 \times 10^{-2} \exp(-0.037x). \quad (3)$$

Research[64] has shown that the nucleation frequency J increases with pressure and the supersaturation. However, the temperature dependence of J has yet to be examined. To check the effect of temperature, we investigated the nucleation of CH_4 + C_3H_8 mixed-gas hydrates (fixed at CH_4:C_3H_8 = 95:5) at 274.3 and 275.4 K. For this purpose, we also examined two σ conditions, approximately 1.0 and 1.2.

In Fig. 3, we plot the resulting nucleation probability distributions. The experimental conditions and the parameter values obtained by fitting the equation (1) to each distribution are listed in Table 2.

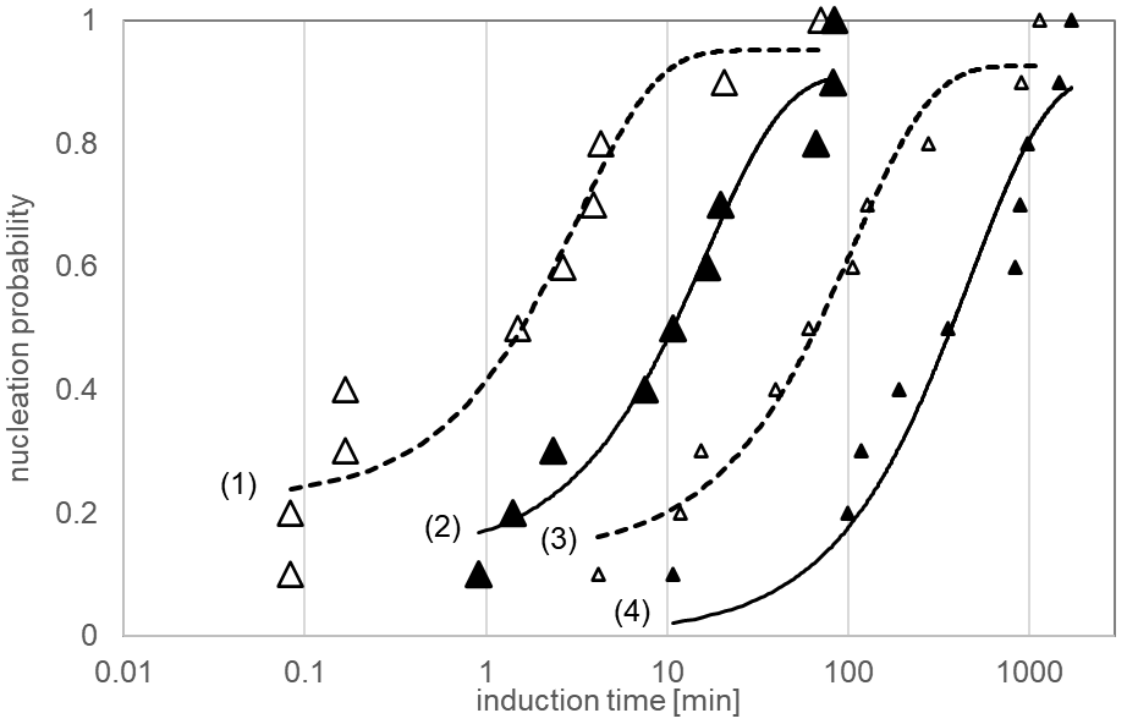

Fig. 3: Nucleation probability distributions $\Pi(t)$ of CH_4 + C_3H_8 (95:5) mixed gas hydrates for four P and T conditions. The values of P, T, and σ are listed in Table 2.

Table 2: Summary of average formation conditions and fitting parameters.

Exp. No.	CH_4	C_3H_8	P_f	T_f	σ	J	$\langle J \rangle$	τ_0	R^2
	%	%	MPa	K		$\times 10^{-3}$ min^{-1}	$\times 10^{-3}$ min^{-1}	min	
(1)	93	7	1.70	275.4	1.27	273	147	–0.92	0.923
(2)	93	7	1.53	275.4	1.04	44.8	40.6	–3.7	0.938
(3)	96	4	1.50	274.3	0.88	7.50	10.5	–21	0.956
(4)	92	8	1.37	274.2	1.24	1.36	0.77	–103	0.950

These results show that for a (nearly) fixed σ, a temperature difference of only 1.1 K results in a difference in the value of $\langle J \rangle$ of nearly two orders of magnitude. For instance, the nucleation frequency for experiment 1 (σ is about 1.25) is about 200 times higher than that of 4. Thus, the nucleation process of mixed-gas hydrates is sensitive to not only supersaturation, but also temperature. The results also show that for a fixed temperature and composition, the nucleation rate increases with supersaturation. This suggests that the relationship in equation (2) holds qualitatively for the nucleation process of mixed-gas hydrates with different compositions. This finding supports our use of equation (2) to adjust J to the σ-corrected value $\langle J \rangle$.

IV. Discussion

The presence of a small amount of C_3H_8 in CH_4 has long been known to promote hydrate nucleation,[1] but this study is the first to show that there is a clear composition dependence on the nucleation frequency (Fig. 2). We now examine the cause of this composition dependence.

Even at gas-phase concentrations as low as 1%, having C_3H_8 present gives the hydrate crystals the sII structure.[72] So, except for the pure CH_4 hydrate case, all hydrate crystals obtained in this study are considered to have the sII structure. For this structure, we assume that the nucleation frequency may depend on the enclathration state of the guest molecules. For structure sII, the number of $5^{12}6^4$ cages (L cages) is half that of the 5^{12} (S cages). A CH_4 molecule can be enclathrated in either S or L cages, whereas a C_3H_8 molecule can only enclathrate in an L cage. Previous studies have also shown that C_3H_8 molecules in the gas phase are preferentially incorporated into hydrate crystals over CH_4 molecules in the sense that the resulting hydrate crystal becomes C_3H_8-rich compared to the gas-phase composition.[1,72] As the gas-phase concentration of CH_4 decreases (i.e., x increases), we expect that the occupancy ratio of S cages with CH_4 molecules to also decrease. From the trend in Fig. 2, we then hypothesize that the value of $\langle J \rangle$ decreases as the proportion of empty S-cages increases.

We calculated the equilibrium occupancy of CH_4 in the S cage θ_S by using the CSMHYD program,[72] and overlaying this θ_S-x curve on the $\langle J \rangle$ versus x plot in Fig. 4. This is fitted by the exponential curve:

$$\theta_S = 0.759 \exp(-0.0295x), \qquad (4)$$

where the fitting has $R^2 = 0.98$. When the gas composition becomes 100% C_3H_8, all small cages will be empty, although the above fit does not completely vanish at x = 100%. Overlaying this θ_S-x curve on the $\langle J \rangle$ versus x plot in Fig. 4 shows good agreement with these two trends.

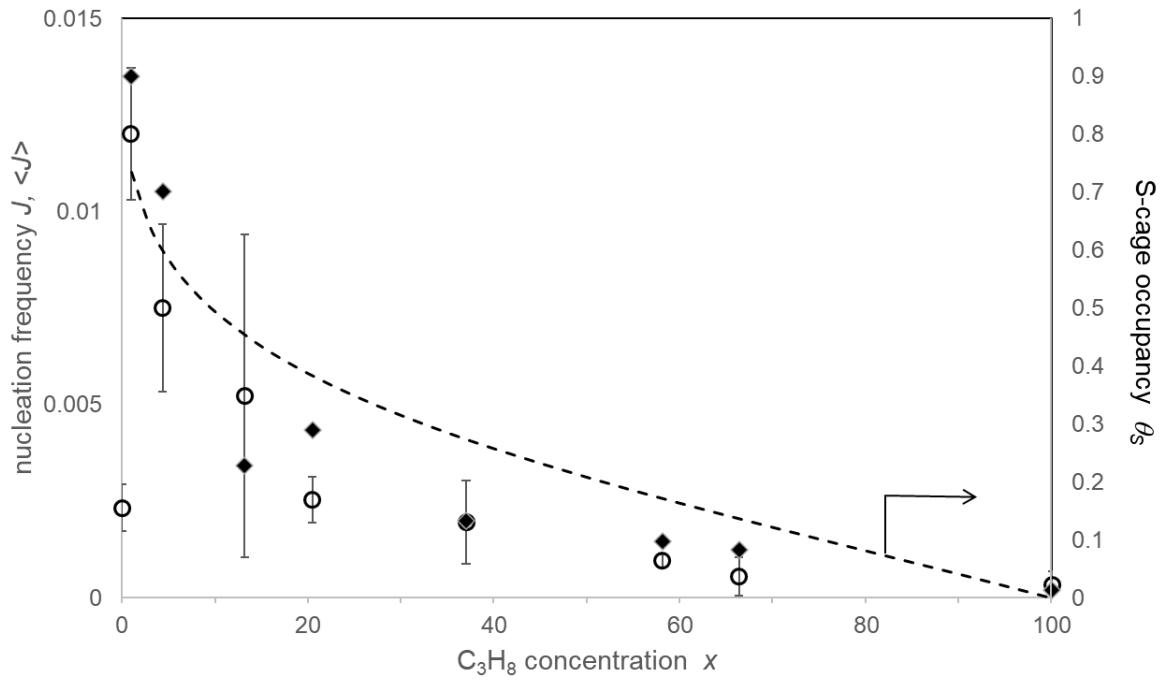

Fig. 4: Dependence of <*J*> and θ_S on the C_3H_8 concentration *x*. Datapoints of *J* (open circles) and <*J*> (solid diamonds) are from Fig. 2 and the dashed line shows the θ_S-*x* curve (right vertical axis).

As the relationship between <*J*> and *x* (equation (3)) can also be approximated with an exponential function, the correlation between <*J*> and θ_S for the mixed-gas hydrate is high (R^2 = 0.95). The good agreement in Fig. 4 indicates that our hypothesis is valid.

For Figs. 2 and 4, the independent variable is the vapor-phase C_3H_8 fraction x, but we also checked whether the results hold when we instead use the estimated fraction of dissolved C_3H_8 in aqueous solution x_{aq}. For the estimate, we assume that the solubilities of CH_4 and C_3H_8 in water at T = 274.7 K and atmospheric pressure are 4.4×10^{-5} and 6.8×10^{-5}, respectively.[75] Assuming that the dissolved amount of a gas type depends linearly on its partial vapor pressure, we estimated the amount of each gas molecule dissolved under the conditions for its formation,

and thus the C_3H_8 concentration in aqueous phase. Upon plotting with x_{aq} instead of x in Fig. 4, the datapoints fit essentially the same curve, so our conclusion above remains unchanged.

Assuming that the nucleation frequency of $CH_4 + C_3H_8$ mixed-gas hydrate is controlled by θ_S, we now examine the nucleation process. Using MD simulations, Zhang et al.[68] found that the t_{ind} of $CH_4 + C_3H_8$ mixed gas hydrate decreases with increasing C_3H_8 concentration in the gas phase, the opposite trend to that found in our measurements. They suggested that the trend results from a considerable time being needed for the formation of stable cages for guest molecules (especially CH_4 molecules). However, their results were not verified experimentally. In contrast, the simulation of pure C_3H_8 hydrate by Chen et al.[69] indicated that the formation of empty cages is equally important to that of guest-occupied cages. The importance of the formation of empty cages during nucleation is also high in the blob hypothesis.[29] As we found here that the nucleation frequency $<J>$ depends on θ_S, or the fraction of cages that are empty $(1-\theta_S)$, our results here qualitatively support the results of these last two studies.

Considering the initial stage of nucleation in the $CH_4 + C_3H_8$ mixed-gas hydrate system, which would be related to the amorphous state in the blob hypothesis,[28,29] the theory predicts that first an L-cage-like structure will form around the dissolved C_3H_8 molecule and then will stabilize, as C_3H_8 occupies only the $5^{12}6^4$ cage. Another simulation has shown that a cage-like structure surrounding a C_3H_8 molecule is formed in the early stage of nucleation, although it would last a relatively short time.[70] On the other hand, as CH_4 can occupy any type of cage in both sI and sII structures, it is possible for any structure to form around the dissolved CH_4 molecule. Hence, wrong (unstable) structures may form first based on the occupation of the CH_4 molecules, thus slowing down the nucleation of the stable phase.[8] As the CH_4 molecules occupy the small cage in the early stage of gas-hydrate formation,[70,76] and the small cage is common to all hydrate structures, the formation of the large cages determine which type of

structure will form in such mixed-gas hydrates. Also, for determining the bulk-hydrate structure, it is important to stabilize the empty S-cage structure not occupied by CH_4.

Based on our experimental results and the above considerations, we propose the overall rate of the mixed-gas hydrate nucleation involves the following individual rates:

(A) How quickly dissolved guest molecules aggregate in water.

(B) How quickly each guest molecule selects the stable cage-like structure.

(C) How quickly the empty-cage structures are stabilized.

After these three processes are completed, the amorphous phase will change to the critical nucleus. The time required for the nucleation is the sum of the times for all three processes, but we expect that one process will be much slower than the others and thus will dominate the time scale. In the case of CH_4 + C_3H_8 mixed-gas hydrate, we expect that at higher C_3H_8 concentrations the timescales of A and B will decrease, but that of C will increase. Furthermore, once CH_4 molecules are arranged at suitable sites, the host structure becomes stable, but the more the empty cages there are, the more difficult it becomes to reach the final structure of the critical nucleus. So, it will take longer to form a critical nucleus if the amorphous phase has a larger number of empty cages. In other words, the formation process of this critical nucleus determines the length of the induction time and thus the magnitude of the nucleation frequency *J*. We argue that this process qualitatively explains the exponential decrease in the nucleation frequency of CH_4 + C_3H_8 mixed-gas hydrate.

Here, we claim that the length of the induction period of CH_4 + C_3H_8 mixed-gas hydrate (sII structure) is mainly controlled by rate C, the stabilizing of the empty 5^{12} cages. Of course, under short t_{ind} conditions, which are the CH_4-rich conditions, the sI-like structure likely forms prior to that of the sII-like structure, which would increase t_{ind}. This may be the reason why the

induction time at 50% nucleation probability slightly increases when the C_3H_8 concentration decreases below about 10% (Fig. 1(b)).

In addition, the nucleation frequency J of mixed-gas hydrate formed with gas of x = 1% is one order of magnitude higher than that of pure CH_4 hydrate, which indicates that the presence of even a small amount of C_3H_8 molecules promotes the gas-hydrate nucleation. For the formation of pure CH_4 hydrate (sI structure), experiments show that CH_4 molecules tend to be included in the 5^{12} cage in the early stage of formation, with the other cage-structures having an energy barrier to formation.[76] If a similar situation applies to the nucleation of CH_4 + C_3H_8 mixed-gas hydrate (sII structure), which contains more 5^{12} cages in the unit cell than that of sI, then it may take less time to form stable nuclei in the system if the CH_4 molecules occupy 5^{12} cages and the C_3H_8 molecules stabilize $5^{12}6^4$ cage-like structures simultaneously in the early stage of nucleation. In this way, the C_3H_8 molecules would act as a stabilizer for the initial amorphous phase formed by CH_4 molecules. According to CSMHYD calculations,[72] the composition in the mixed-gas hydrate under equilibrium conditions with gas of x = 1% is CH_4: C_3H_8 = 67:33, which is close to the ratio of 5^{12} cages and $5^{12}6^4$ cages in the sII structure. Therefore, this is the composition at which CH_4 molecules occupy all 5^{12} cages and C_3H_8 molecules occupy remaining $5^{12}6^4$ cages —that is, the two gases are separated by cage type. We argue that this condition allows the initial amorphous phase formed by the aggregation of guest molecules to quickly stabilize, requiring the shortest time to complete process B and thus maximizing the nucleation frequency J.

Although we have argued that C_3H_8 molecules promote the formation of mixed-gas hydrates, the same can also be said for CH_4. As shown in Fig. 2, the more CH_4 is contained in the mixed-gas phase, the larger the value of J becomes over that for pure C_3H_8 hydrate. This

clearly indicates that CH_4 molecules also promote the formation of mixed-gas hydrates. Moreover, in this case, the promotion holds true at all concentrations.

On the other hand, classical nucleation theory[12,77-79] predicts that the size of the critical nucleus increases with increasing temperature, thus increasing the energy barrier. So, the nucleation frequency J may decrease (i.e., increase t_{ind}) at higher temperature. However, as shown in Fig. 3 and Table 2, we found the opposite trend, specifically that the value of J for mixed-gas hydrates to be larger at higher temperature T. Therefore, we consider that the "induction time" observed experimentally involves not only the formation of the critical nuclei (A to C above), but also the time for the crystals to grow large enough to detect experimentally. If so, the nucleation frequency observed experimentally should be determined by the following rates:

(D) How quickly a sufficient number of critical nuclei form in the system

(E) How fast the initial crystal growth induces a measurable temperature rise or pressure drop

For the processes of (A) to (C), the time to reach a stable structure should be shorter at higher temperature because the frequency of molecular reorganization within the amorphous phase should be faster. For (D) and (E), the growth process of the macroscopic crystal structure is thought to be a thermally activated process and thus should also be faster at higher temperature. Unfortunately, we cannot accurately estimate the T dependence from only two T points and two σ conditions. Nevertheless, we roughly estimated the activation energies in this T range to be about 75 kJ/mol when $\sigma \approx 1.2$ and about 17 kJ/mol when $\sigma \approx 0.9$. These values are within an order of magnitude of that for the hydrogen bond energy of ice Ih (about 28 kJ/mol[80]). If we assume that the activation energy for bulk crystal growth of $CH_4 + C_3H_8$ mixed gas hydrate is similar to that of pure CH_4 hydrate ($1.1–1.9 \times 10^2$ kJ/mol[3,81-82]), then the activation energy for

the structure-formation process from the amorphous phase to a small crystal structure is one order of magnitude smaller. Thus, this nucleation process differs from the subsequent bulk growth process of the mixed-gas hydrate crystal.

V. Conclusions

We measured the induction times of CH_4 + C_3H_8 mixed-gas hydrate at about 274 K and a range of compositions, finding them to be shorter than those of both pure hydrates. The composition dependence of the nucleation frequency of CH_4 + C_3H_8 mixed-gas hydrate exponentially increased with increasing CH_4 concentration. By increasing the temperature 1 K at a fixed composition and supersaturation, we found the nucleation frequency to increase by about one order of magnitude.

Since the composition dependence of nucleation frequency is similar to that of the empty-cage ratio, we argued that the nucleation rate is controlled by the time required for the construction of stable empty cages. Based on these experimental results, we proposed a nucleation process of mixed-gas hydrates. In this model, the initial structure of mixed-gas hydrate is the amorphous phase that contains C_3H_8-containing $5^{12}6^4$ cage-like clusters, CH_4-containing 5^{12} cage-like clusters, and empty-cage-like aggregates. In addition, the temperature dependence of the nucleation frequency suggests that the experimentally obtained induction time includes not only the critical-nucleus formation process, but also the time for the crystals to grow large enough to be observed experimentally (e.g., by a temperature rise or a pressure drop). This model will need to be tested through experimental studies, including spectroscopy, as well as with simulation studies.

If nucleation of gas hydrate is such a two-step formation process, then it is not yet possible to fully understand its nucleation process because molecular-dynamic simulations cannot calculate over the experimental timescales (minutes to hours), whereas experiments cannot discern the short timescales in the simulations (pico- to nano-seconds). However, the results of this study strongly suggest the possibility that the empty-cage formation process controls the bulk crystal formation process in the early stage of nucleation, and therefore experimental results can help fill the knowledge gap between these two approaches.

AUTHOR INFORMATION

Corresponding Author

E-mail: t-uchida@eng.hokudai.ac.jp (T. U.), orcid.org/0000-0003-2304-376X

Author Contributions

T. U., M. H. and K. Y. conceived the idea and designed the study. M. H. and T. U. performed the sample preparations and the formation tests, M. O. verified the sample compositions, and M. H. and T. U. analyzed the nucleation data. T. U. wrote the original draft of manuscript. All the authors contributed to review and editing on the manuscript.

Funding Sources

This work is partly supported financially by the Arai Foundation.

Notes

Any additional relevant notes should be placed here.

ACKNOWLEDGMENT

This work is partly supported by the joint project with AIST Hokkaido. The authors acknowledge the fruitful discussion in the Joint Research Program of the Institute of Low Temperature Science, Hokkaido University (24S002). We would also like to thank Dr. J. Nelson, the editor of Redmond Physical Sciences (www.redmondphysicalsciences.com) for the English language review.

ABBREVIATIONS

CSMHYD: the name of software that predicts the thermodynamics of stable hydrate structures at given pressure, temperature, and composition conditions.

AUTHOR DECLARATIONS

Conflict of Interest

The authors have no conflicts to disclose.

DATA AVAILABILITY

The data that support the findings of this study are available from the corresponding author upon reasonable request.

REFERENCES

(1) Sloan, E.D.; Koh, C.A. Clathrate hydrates of natural gases, 3rd ed.; CRC Press: Boca Raton, FL, 2007, p.752. doi: 10.1201/9781420008494.

(2) Ripmeester, J.A.; Alavi, S. Some current challenges in clathrate hydrate science: nucleation, decomposition and the memory effect. *Curr. Opin. Solid State Mater. Sci.* **2016**, 20, 344-351. Doi: 10.1016/j.cossms.2016.03.005

(3) Vysniauskas, A.; Bishnoi, P. R. A Kinetic Study of Methane Hydrate Formation, *Chem. Eng. Sci.* **1983**, 38 (7), 1061-1072. DOI: 10.1016/0009-2509(83)80027-X

(4) Englezos, P.; Kalogerakis, N.; Dholabhai, P. D.; Bishnoi, P. R. Kinetics of Gas Hydrate Formation from Mixtures of Methane and Ethane, *Chem. Eng. Sci.* **1987**, 42 (11), 2659-2666. DOI: 10.1016/0009-2509(87)87016-1

(5) Englezos, P.; Kalogerakis, N.; Dholabhai, P. D.; Bishnoi, P. R. Formation and Decomposition of Gas Hydrates of Natural Gas Components, *J. Inclusion Phenomena and Molecular Recognition in Chemistry* **1990**, 8, 89-101. DOI: 10.1007/BF01131290

(6) Bishnoi, P. R.; Natarajan, V. Formation and Decomposition of Gas Hydrates, *Fluid Phase Equilibria* **1996**, 117 (1-2) 168-177. DOI: 10.1016/0378-3812(95)02950-8

(7) Lee, J. D.; Susilo, R.; Englezos, P. Methane-ethane and methane-propane hydrate formation and decomposition on water droplets, *Chem. Eng. Sci.* **2005**, 60 (15), 4203-4212. DOI: 10.1016/j.ces.2005.03.003

(8) Ripmeester, J. A. Improving Our Understanding of Gas Hydrate Formation Processes: The Importance of Multi-Technique Approaches, in *Physics and Chemistry of Ice* (ed. W. F. Kuhs), RSC Publishing, Cambridge, U.K., 2007, p. 59-71.

(9) Ribeiro, C. P.; Lage, P. L. C. Modelling of hydrate formation kinetics: State-of-the-art and future directions, *Chem. Eng. Sci.* **2008**, 63 (8), 2007-2034. DOI: 10.1016/j.ces.2008.01.014

(10) Kummer, R.; Linga, P.; Moudrakovski, I.; Ripmeester, J. A.; Englezos, P. Structure and Kinetics of Gas Hydrates from Methane/Ethane/Propane Mixtures Relevant to the Design of Natural Gas Hydrate Storage and Transport Facilities, *AIChE J.* **2008**, 54 (8), 2132-2144. DOI: 10.1002/aic.11527

(11) Maghsoodloo Babakhani, S.; Bouillot, B.; Douzet, J.; Ho-Van, S.; Herri, J. M. A new approach of studying mixed gas hydrates involving propane at non-equilibrium

conditions and final state: An experimental study and modeling, *Chem. Eng. Sci.* **2018**, 179, 150160. DOI: 10.1016/j.ces.2018.01.017

(12) Englezos, P.; Alavi, S.; Ripmeester, J. A. Kinetics of Clathrate Hydrate Processes, in *Clathrate Hydrates: Molecular Science and Characterization* (eds. J. A. Ripmeester and S. Alavi) WILEY--VCH GmbH, Weinheim, Germany, 2022, vol. 2, p.631-716

(13) Klapproth, A.; Piltz, R. O.; Kennedy, S. J.; Kozielski, K. A. Kinetics of sII and Mixed sI/sII, Gas Hydrate Growth for a Methane/Propane Mixture Using Neutron Diffraction. *J. Phys. Chem. C* **2019**, 123, 2703−2715. DOI: 10.1021/acs.jpcc.8b06693

(14) Menezes, D. E. S.; Sum, A. K.; Desmedt, A.; Pessôa Filho, P. A.; Robustillo Fuentes, M. D. Coexistence of sI and sII in methane-propane hydrate former systems at high pressures, *Chem. Eng. Sci.* **2019**, 208, 115149. DOI: 10.1016/j.ces.2019.08.007

(15) Schicks, J. M.; Naumann, R.; Erzinger, J.; Hester, K. C.; Koh, C. A.; Sloan, E. D. Phase Transitions in Mixed Gas Hydrates: Experimental Observations versus Calculated Data. *J. Phys. Chem. B* **2006**, 110, 11468−11474.

(16) Uchida, T.; Takeya, S.; Kamata, Y.; Ohmura, R.; Narita, H. Spectroscopic measurements on binary, ternary, and quaternary mixed-gas molecules in clathrate structures, *Ind. & Eng. Chem. Res.,* **2007**, 46 (14), 5080-5087. DOI:10.1021/ie070153w

(17) Natarajan, V.; Bishnoi, P. R.; Kalogerakis, N. Induction phenomena in gas hydrate nucleation". *Chem. Eng. Sci.* **1994**, 49 (13), 2075-2087. DOI 10.1016/0009-2509(94)E0026-M

(18) Khurana, M.; Yin, Z.; Linga, P. A review of clathrate hydrate nucleation. *ACS Sustainable Chem. Eng.* **2017**, 5 (12), 11176-11203. DOI: 10.1021/acssuschemeng.7b03238

(19) Cho, S. J.; Hai, T. L. S.; Lee, J. D., In-situ Raman and kinetic study on the methane hydrate formation and decomposition, *Energy Procedia* **2019**, 158, 5615-5621. DOI: 10.1016/j.egypro.2019.01.578

(20) Maeda, N.; Wells, D.; Becker, N.C.; Hartley, .G.; Wilson, P.W.; Haymet, A.D.J.; Kozielski, K.A. Development of a high pressure automated lag time apparatus for experimental studies and statistical analyses of nucleation and growth of gas hydrates. *Rev. Sci. Instruments* **2011**, 82, 065109-1-7. Doi: 10.1063/1.3602926

(21) Maeda, N. Nucleation curves of model natural gas hydrates on a quasi-free water droplet. *AIChE J.* **2015**, 61 (8) 2611-2617. Doi: 10.1002/aic.14898

(22) English, N. J.; MacEloy, J. M. D., Perspectives on molecular simulation of clathrate hydrates: Progress, prospects and challenges, *Chem. Eng. Sci.* **2015**, 121, 133-156. DOI: 10.1016/j.ces.2014.07.047

(23) Sloan, E. D.; Fleyfel, F. A. Molecular mechanism for gas hydrate nucleation from ice, *AIChE J.* **1991**, 37 (9), 1281-1292. DOI: 10.1002/aic.690370902

(24) Christiansen, R. L.; Sloan, E. D. Mechanisms and kinetics of hydrate formation. *Ann. N. Y. Acad. Sci.* **1994**, *715* (1), 283−305. DOI: 10.1111/j.1749-6632.1994.tb38841.x

(25) Long, J. *Gas Hydrate Formation Mechanism and Kinetic Inhibition*; Colerado School of Mines, 1994.

(26) Kvamme, B. A. New Theory for the Kinetics of Hydrate Formation. In *Proceedings of 2nd International Conference on Natural Gas Hydrates*, Monfort, J. P., Ed.; 1996; p 139.

(27) Radhakrishnan, R.; Trout, B. L. A new approach for studying nucleation phenomena using molecular simulations: application to CO_2 hydrate clathrates. *J. Chem. Phys.* **2002**, 117 (4), 1786−1796. DOI: 10.1063/1.1485962

(28) Jacobson, L. C.; Hujo, W.; Molinero, V. Amorphous precursors in the nucleation of clathrate hydrates. *J. Am. Chem. Soc.* **2010**, 132 (33), 11806−11811. DOI: 10.1021/ja1051445

(29) Jacobson, L. C.; Hujo, W.; Molinero, V. Nucleation pathways of clathrate hydrates: effect of guest size and solubility. *J. Phys. Chem. B* **2010**, 114 (43), 13796−13807. DOI: 10.1021/jp107269q

(30) Vatamanu, J.; Kusalik, P. G. Observation of two-step nucleation in methane hydrates. *Phys. Chem. Chem. Phys.* **2010**, 12 (45), 15065−15072. DOI: 10.1039/C0CP00551G

(31) Lauricella, M.; Meloni, S.; English, N. J.; Peters, B.; Ciccotti, G. Methane clathrate hydrate nucleation mechanism by advanced molecular simulations. *J. Phys. Chem. C* **2014**, 118 (40), 22847−22857. DOI: 10.1021/jp5052479

(32) He, Z.; Linga, P.; Jiang, J. What are the key factors governing the nucleation of CO_2 hydrate? *Phys. Chem. Chem. Phys.* **2017**, 19 (24), 15657−15661. DOI: 10.1039/C7CP01350G

(33) Bai, D.; Chen, G.; Zhang, X.; Wang, W. Nucleation of the CO_2 hydrate from three-phase contact lines. *Langmuir* **2012**, 28 (20), 7730−7736. DOI: 10.1021/la300647s

(34) Karaaslan, U.; Parlaktuna, M. Surfactants as Hydrate Promoters? *Energy Fuels* **2000**, 14 (5), 1103−1107. DOI: 10.1021/ef000069s

(35) Kumar, A.; Bhattacharjee, G.; Kulkarni, B. D.; Kumar, R. Role of Surfactants in Promoting Gas Hydrate Formation. *Ind. Eng. Chem. Res.* **2015**, 54 (49), 12217−12232. DOI: 10.1021/acs.iecr.5b03476.

(36) Sa, J.-H.; Sum, A.K. Promoting Gas Hydrate Formation with Ice-Nucleating Additives for Hydrate-Based Application. *Appl. Energy* **2019**, 251, 113352. DOI: 10.1016/j.apenergy.2019.113352.

(37) Majid, A.A.A.; Worley, J.; Koh, C.A. Thermodynamic and kinetic promoters for gas hydrate technological applications. *Energy Fuels* **2021**, 35, 19288-19301. DOI: 10.1021/acs.energyfuels.1c02786

(38) Chaturvedi, E.; Laik, S.; Mandal, A. A Comprehensive Review of the Effect of Different Kinetic Promoters on Methane Hydrate Formation. *Chinese J. Chem. Eng*. **2021**, 32, 1-16. DOI: 10.1016/j.cjche.2020.09.027.

(39) Wang, F.; Song, F.-P.; Li, C.; Sun, M.-T. Preparation of a Hydrogel-Based Promoter for Methane Hydrate Formation: Effects of $-SO_3^-$ Density on Promotion Efficiency. *Energy Fuels* **2022**, 36, 2731-2738. DOI: 10.1021/acs.energyfuels.1c04040

(40) Liu, Z.; Pan, Z.; Zhang, Z.; Liu, P.; Shang, L.; Li, B. Effect of Porous Media and Sodium Dodecyl Sulphate Complex System on Methane Hydrate Formation. *Energy Fuels* **2018**, 32, 5736-5749. DOI: 10.1021/acs.energyfuels.8b00041

(41) Song, Y.; Wang, F.; Liu, G.; Luo, S.; Guo, R. Promotion Effect of Carbon Nanotubes-Doped SDS on Methane Hydrate Formation. *Energy Fuels* **2017**, 31, 1850−1857. DOI: 10.1021/acs.energyfuels.6b02418.

(42) Zhou, S.-D.; Yu, Y.-S.: Zhao, M.-M.; Wang, S.-L.; Zhang, G.-Z. Effect of Graphite Nanoparticles on Promoting CO_2 Hydrate Formation. *Energy Fuel* **2014**, 28, 4694-4698. DOI: 10.1021/ef5000886

(43) Nashed, O.; Lal, B.; Partoon, B.; Sabil, K. M.; Hamed, Y. Kinematic Study of Methane Hydrate Formation and Self-Preservation in the Presence of Functionalized Carbon Nanotubes. *Energy Fuels* **2019**, 33, 7684-7695. DOI: 10.1021/acs.energyfuels.9b01531.

(44) McElligott, A.; Uddin, H.; Meunier, J.-L.; Servio, P. Effects of Hydrophobic and Hydrophilic Graphene Nanoflakes on Methane Hydrate Kinetics. *Energy Fuels* **2019**, 33, 11705-11711. DOI: 10.1021/acs.energyfuels.9b02927

(45) Sun, M.-T.; Zhang, G.-D.; Wang, F. Graphene-based kinetic promotion of gas hydrate formation. *Front. Chem.* **2020**, 8, 481. DOI: 10.3389/fchem.2020.00481

(46) Nguyen, N. N.; Galib, M.; Nguyen, A. V. Critical Review on Gas Hydrate Formation at Solid Surfaces and in Confined Spaces-Why and How Does Interfacial Regime Matter? *Energy Fuels* **2020**, 34, 6751−6760. DOI: 10.1021/acs.energyfuels.0c01291.

(47) Mohammed, S.; Asgar, H.; Deo, M.; Gadikota, G. Interfacial and Confinement-Mediated Organization of Gas Hydrates, Water, Organic Fluids, and Nanoparticles for the Utilization of Subsurface Energy and Geological Resources. *Energy Fuel* **2021**, 35, 4687-4710. DOI: 10.1021/acs.energyfuels.0c04287

(48) Machida, H.; Sugahara, T.; Hirasawa, I. The Moment of Initial Crystallization Captured on Functionalized Nanoparticles. *Comm. Material.* **2021**, 2, 66. DOI: 10.1038/s43246-021-00171-w.

(49) Qin, Y.; Pan, Z.; Liu, Z.; Shang, L.; Zhou, L. Influence of the Particle Size of Porous Media on the Formation of Natural Gas Hydrate: A Review. Energy Fuels 2021, 35,

11640-11664. Doi: 10.1021/acs.energyfuels.1c00936Rong, W.; Zhang, Y.; Luo, S.; Guo, R. Promotion Effect of Copper Nanowire-Doped SDS in Methane Hydrate Formation. *Energy Fuels* **2022**, 36, 4880-4887. DOI: 10.1021/acs.energyfuels.1c04406

(50) May, E.F.; Wu. R.; Kelland, M.A.; Aman, Z.M.; Kozielski, K.A.; Hartley, P.G.; Maeda, N. Quantitative kinetic inhibitor comparisons and memory effect measurements from hydrate formation probability distribution. *Chem. Eng. Sci.* **2014**, 107, 1-12. DOI: 10.1016/j.ces.2013.11.048

(51) Sowa, B.; Maeda, N. Statistical study of the memory effect in model natural gas hydrate systems. *J. Phys. Chem. A* **2015**, 119, 10784-10790. DOI: 10.1021/acs.jpca.5b07308

(52) Maeda, N. Interfacial Nanobubbles and the Memory Effect of Natural Gas Hydrates. *J. Phys. Chem. C* **2018**, 122, 11399−11406. DOI: 10.1021/acs.jpcc.8b02416

(53) Kou, X. ; Feng, J.-C.; Li, X.-S.; Wang, Y.; Chen, Z.-Y. Memory effect of gas hydrate: Influencing factors of hydrate reformation and dissociation behaviors, *Appl. Energy* **2022**, 306, 118015. DOI: 10.1016/j.apenergy.2021.118015

(54) Uchida, T.; Sugibuchi, R.; Yamazaki, K.; Gohara, K. Nucleation behavior of single-gas hydrates in the batch-type stirred reactor and their promotion effect with ultrafine bubbles: a mini review and perspectives, *Energy Fuels* **2022**, 36, 10444-10457. DOI: 10.1021/acs.energyfuels.2c01403

(55) Wei, Y.; Maeda, N. Mechanisms of the memory effect of clathrate hydrates, *Chem. Eng. Sci.* **2023**, 270, 118538. DOI: 10.1016/j.ces.2023.118538

(56) Kuang, Y.; Li, W.; Lin, Z.; Zheng, Y.; Craig, V. S. J. Experimental Study on Memory Effect of Gas Hydrates: Interaction between Micronanobubbles and Solute Molecules, *J. Phys. Chem. C* **2024**, 128, 16237-16249. DOI: 10.1021/acs.jpcc.4c05186

(57) Makogon, Y. F. *Hydrates of Hydrocarbons*; Pennwell Books, 1997.

(58) Sloan, E. D.; Subramanian, S.; Matthews, P. N.; Lederhos, J. P.; Khokhar, A. A. Quantifying Hydrate Formation and Kinetic Inhibition. *Ind. Eng. Chem. Res.* **1998**, 37 (8), 3124−3132. DOI: 10.1021/ie970902h

(59) Rodger, P. M. Methane hydrate: melting and memory. *Ann. N. Y. Acad. Sci.* **2000**, 912 (1), 474−482. DOI: 10.1111/j.1749-6632.2000.tb06802.x

(60) Uchida, T.; Yamazaki, K.; Gohara, K. Generation of micro- and nano-bubbles in water by dissociation of gas hydrates. *Korean J. Chem. Eng.* **2016**, 33 (5), 1749-1755. DOI: 10.1007/s11814-016-0032-7

(61) Uchida, T.; Yamazaki, K.; Gohara, K. Gas nanobubbles as nucleation acceleration in the gas-hydrate memory effect. *J. Phys. Chem. C* **2018**, 120 (47), 2662026629. DOI: 10.1021/acs.jpcc.6b07995

(62) Uchida, T.; Miyoshi, H.; Sugibuchi, R.; Suzuta, A.; Yamazaki, K.; Gohara, K. Contribution of ultra-fine bubbles to promoting effect on propane hydrate formation. *Front. Chem.* **2020**, 8, 480. DOI: 10.3389/fchem.2020.00480

(63) Uchida, T.; Miyoshi, H.; Yamazaki, K.; Gohara, K. Promoting effect of ultra-fine bubbles on CO_2 hydrate formation. *Energies* **2021**, 14, 3386. DOI: 10.3390/ en14123386

(64) Uchida, T.; Sugibuchi, R.; Hayama, M.; Yamazaki, K. Supersaturation dependent nucleation of methane + propane mixed-gas hydrate, *J. Chem. Phys.* **2024**, 160 (7), 074502. DOI: 10.1063/5.0189967

(65) Smith, C.; Pack, D.; Barifcani, A. Propane, n-butane and i-butane stabilization effects on methane gas hydrates, *J. Chem. Thermodyn.* **2017**, 115, 293-301. DOI: 10.1016/j.jct.2017.08.013

(66) Uchida, T.; Hirano, T.; Ebinuma, T.; Narita, H.; Gohara, K.; Mae, S.; Matsumoto, R. Raman Spectroscopic Determination of Hydration Number of Methane Hydrates, *AIChE Journal* **1999**, 45 (12), 2641-2645. DOI: 10.1002/aic.690451220

(67) Li, Y.; Wu, N.; He, C. Q.; Sun, Z.; Zhang, Z.; Hao, X.; Chen, Q.; Bu, Q.; Liu, C.; Sun, J. Nucleation probability and memory effect of methane-propane mixed gas hydrate, *Fuel* **2021**, 291, 120103. DOI: 10.1016/j.fuel.2020.120103

(68) Zhang, Z.; Guo, G.-J.; Wu, N.; Kusalik, P. G. Molecular Insights into Guest and Composition Dependence of Mixed Hydrate Nucleation, *J. Phys. Chem. C* **2020**, 124, 25078-25086. DOI: 10.1021/acs.jpcc.0c07375

(69) Chen, Y.; Chen, C.; Sum, A. K. Propane and Water: The Cooperativity of Unlikely Molecules to Form Clathrate Structures. *J. Phys. Chem. B* **2020**, 124, 4661−4671. DOI: 10.1021/acs.jpcb.0c02675

(70) Chen, Y.; Chen, C.; Sum, A. K., Molecular Resolution into the Nucleation and Crystal Growth of Clathrate Hydrates Formed from Methane and Propane Mixtures, *Cryst. Growth Des*. **2021**, 21, 960-973. DOI: 10.1021/acs.cgd.0c01303

(71) Chen, Y.; Takeya, S.; Sum, A.S. Topological dual and extended relations between networks of clathrate hydrates and Frank-Kasper phases, *Nat. Commun.* **2023**, 14, 596. DOI: 10.1038/s41467-023-36242-4

(72) Sloan, E. D. Jr. Clathrate hydrates of natural gases, 2nd ed. Revised and Expanded; CRC Press: Boca Raton, FL, 1998, p.705.

(73) Toschev, S.; Milchev, A.; Stoyanov, S. On some probabilistic aspects of the nucleation process. *J. Crystal Growth* **1972**, 13/14, 123-127. DOI: 10.1016/0022-0248(72)90073-5

(74) Takeya, S.; Hori, A.; Hondoh, T.; Uchida, T. Freezing-memory effect of water on nucleation of CO2 hydrate crystals. *J. Phys. Chem. B* **2000**, 104, 4164-4168. DOI: 10.1021/jp993759+

(75) The Chemical Society of Japan. Kagaku-Binran (Handbook of Chemistry), 5th ed.; Fundamental; Maruzen Co. Ltd.: Tokyo, Japan, **2004**, II-144-149.

(76) Schicks, J. M.; Luzi-Helbing, M. Cage occupancy and structural changes during hydrate formation from initial stages to resulting hydrate phase, *Spectrochim. Acta. A: Molecul. Biomolecul. Spectro.* **2015**, 115, 528-536. DOI: 10.1016/j.saa.2013.06.065

(77) Kashchiev, D.; Firoozabadi, A. Nucleation of gas hydrates, *J. Crystal Growth* **2002**, 243, 476-489. DOI: 10.1016/S0022-0248(02)01576-2

(78) Kashchiev, D.; Firoozabadi, A. Induction time in crystallization of gas hydrates, *J. Crystal Growth* **2003**, 250, 499-515. DOI: 10.1016/S0022-0248(02)02461-2

(79) Ke, W.; Svartaas, T. M.; Chen, D. A review of gas hydrate nucleation theories and growth models, *J. Nat. Gas Sci. Eng.* **2019**, 61, 169-196. DOI: 10.1016/j.jngse.2018.10.021

(80) Hobbs, P. V. *Ice Physics*; Oxford Univ. Press, NY, 1974, p. 837.

(81) Freer, E. M.; Selim, M. S.; Sloan, E. D. Jr., Methane hydrate film growth kinetics, *Fluid Phase Eq.* **2001**, 185, 65-75. DOI: 10.1016/S0378-3812(01)00457-5

(82) Bian, H.; Ai, L.; Heng, J. Y. Y.; Maitland, G. C.; Hellgardt, K. Effects of chemical potential differences on methane hydrate formation kinetics, *Chem. Eng. J.* **2023**, 452 (2), 139084. DOI: 10.1016/j.cej.2022.139084

TOC graphic

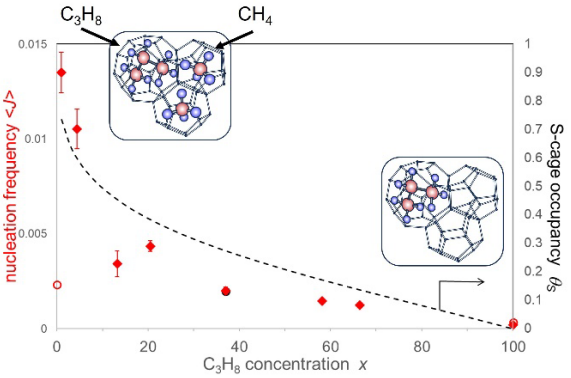
C3H8
CH4
0.015
0.01
0.005
0
nucleation frequency </>
1
0.9
0.8
0.7
0.6
0.5
0.4
0.3
0.2
0.1
0
S-cage occupancy θS
0
20
40
60
80
100
C3H8 concentration x